Proceedings World Geothermal Congress 2020+1
Reykjavik, Iceland, April - October 2021

MT resistivity structure at Abijata and Shalla geothermal field, southern main Ethiopian rift Geothermal Prospect

Kebede M. NEGATU

Geological Survey of Ethiopia

kebedeme29@gmail.com

Keywords: Magnetotelluric(MT), 2-D model, Abijata and Shalla resistivity, Anomaly.

ABSTRACT

The Abijata and Shalla Lake is one of the geothermal prospects in the Lakes districts of the main Ethiopian rift (MER), which about 220 km south west of Addis Ababa. The Abijata and Shalla prospect area lies between 7º25'N and 38º30'E, and on the elevation of 1570m above sea level. The lake has no surface outlet and receives the discharge from Lake Ziway, Langano and Abijata. Many hot and warm springs emerge along its eastern, southern and western shores due to the temperature survey. The most important and boiling thermal springs located at the eastern part of the shore.

Due to those to all in the above information electromagnetic methods (EM) are frequently used in the exploration of Geothermal resources for determining the spatial distribution of electrical resistivity (conductivity). Magnetotellurics (MT) and time domain electromagnetic (TDEM) methods are especially used for geothermal exploration when using EM methods. Geothermal resources are ideal targets for EM methods since they produce strong variations in underground electrical resistivity (conductivity). Electrical resistivity is directly related to parameters that characterize geothermal systems. In this report, the application of TEM and MT methods and interpretation of data from the Abijata and Shalla geothermal field in Ethiopia are discussed. MT data were analyzed and modeled using 2-D Occam inversion of the rotationally invariant impedance tensor by rotating the MT data N 35^0 E using the strike direction.

The Bahr skew, swift skew and elliptical representation between 0.003 s to 1 s and 100 s to 1000 s shows the MT data has 2-D/1-D character. The 2-D inversion result shows a low resistivity at shallow depth is interpreted as a sedimentary formation, lateral flow of geothermal fluids or a fracture zone. The existence of clay minerals, especially smectite makes the region below the resistive unaltered layer very conductive. In the region, the temperature is getting high and the most common alteration products are smectite and illite. The unaltered zone is a region where the hot geothermal fluid does not affect the rocks near the surface and the temperature is low. The high resistivity below the low resistivity can be associated with less permeable. The up-flow permeable region below the conductive clay zone is considered the geothermal reservoir in such high-enthalpy geothermal systems and is characterized by high resistivity due to the formation of secondary minerals like chlorite and epidote. Generally, from the 2-D inversion model three main resistivity layers are recognized: a shallow depth relatively thin high-resistivity layer around the stations (100 Ωm), a conductive layer probably the cap rock with resistivity below 10 Ωm, the third resistive zone with high resistivity value (> 100 Ωm).

1. INTRODUCTION AND BACKGROUND

The study area located in the Hosaena map sheet, specifically in the central Main Ethiopian Rift (MER). On the basis of morphology and drainage type, the area is divided into the following physiographic divisions: Central Main Ethiopian Rift and Rift Escarpments. The Main Ethiopian Rift constitutes an area characterized by active extensional tectonics with an E-W oriented direction of extension and the two main fault systems have been identified in the main Ethiopia Rift (MER) NE-SW trending fault system which characterizes the rift margins, and a NNE-SSW trending fault system which is the Wonji fault belt (WFB). On Figure 1, black lines denote border and Wonji faults based on the fault database from Agostini *et al.* (2011), (Corti 2009). The study area bounded by lake Shalla, Abijata and Langano in the central MER which are surrounded by Pleistocene to Holocene pyroclastics and lake sediments. The Rift escarpments and adjacent plateau found along both sides of the rift and it is characterized by different central volcanic complexes. Ignimbrite of the Nazreth group and Dino formations are also found. It commonly has a down ward stepping topography.

In the Shalla-Abijata geothermal field 15 MT soundings were collected by Geological Survey of Ethiopia to delineate the sub surface structure and the reservoir considering the dimensional analysis. The MT data recorded with period ranges 0.003 s to 1000 s with a remote reference (Fig.1). The MT data were processed using the robust processing program SSMT2000 (Phoenix Geophysics Ltd) similar to (Egbert, 1997; Smirnov, 2003). The cross-powers were then graphically edited by the MT editor program to remove the noisy data points and generate “smooth” curves for both phase and apparent resistivity. Most of sounding data has good quality and can be used for interpretation up to the period of 1000 s.

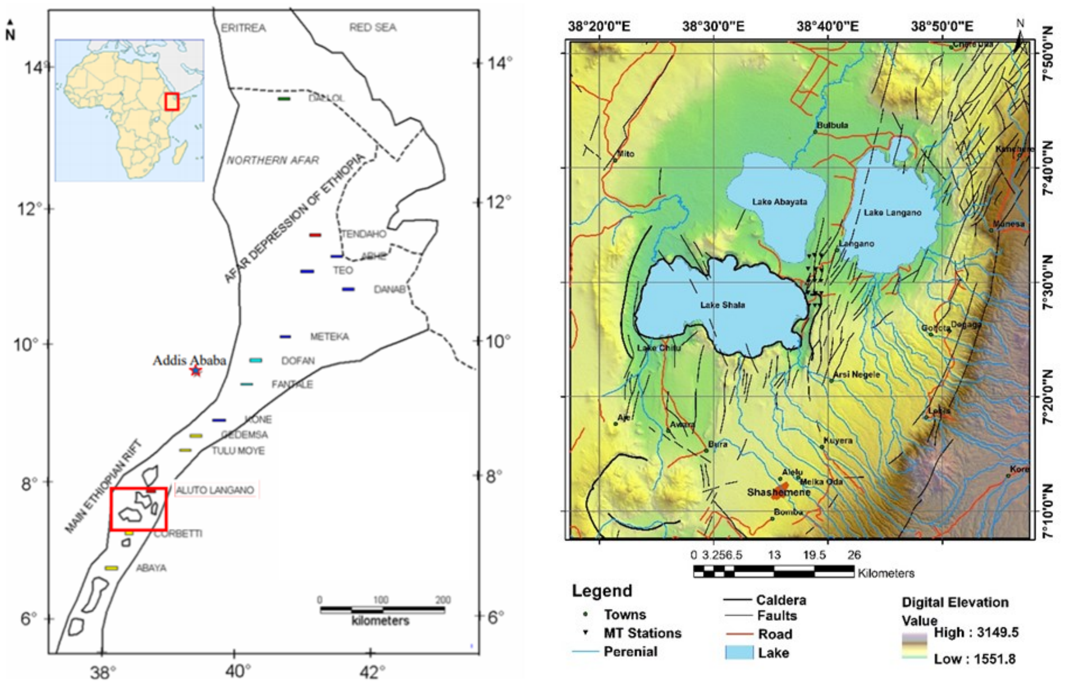

Figure 1: The Main Ethiopian Rift system looking for the geothermal sites (left) and the physiographic map including the structures and the drainage system in the study area.

In this study the dimensionality analysis processed to check the MT data behavior and 2-D inversion models of the rotationally invariant of impedance tensor of MT data was done using Occam program (Constable et al., 1987). Figure 2 shows all MT sounding curves of apparent resistivity and the phase curves. The tendency of these sounding curves indicates volcanic rocks and/or sediment deposit at the surface then, the resistivity decreases due to alteration minerals and the high resistivity unaltered basaltic structure continues and the resistivity decreases in the deepest.

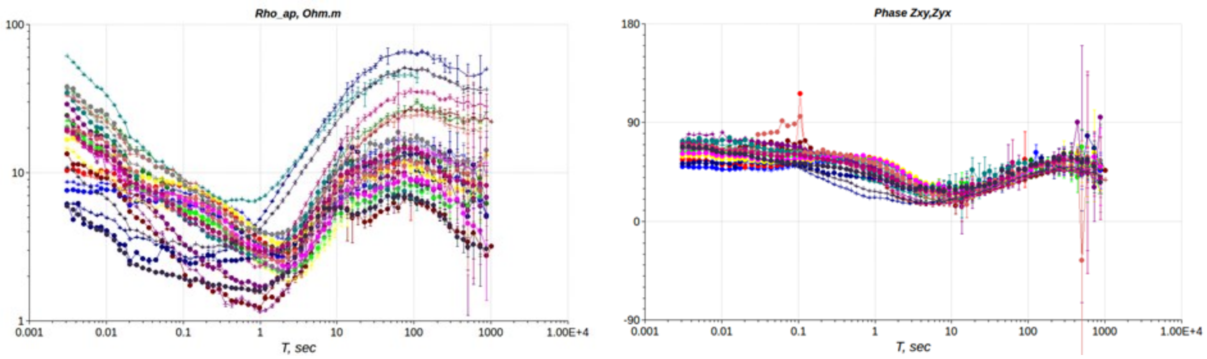

Figure 2: All of MT apparent resistivity and phase curves for TE and TM.

Magnetotelluric method is a natural source (passive) electromagnetic geophysical method that images the electrical properties of the earth. Natural variations in the earth´s magnetic field induce electric field (telluric currents) under the earth´s surface. Depending on signal frequency and resistivity of penetrated material, the MT method can resolve geo-electric structures from depths of tens of meters to depths of hundreds of kilometres (Vozoff, 1991).

2. GEOLOGICAL AND TECTONIC SETTING

The study area, Shalla-Abayata geothermal site is located in the central part of the MER, south of the Afar depression. The MER separates the Nubian and the Somalian plate, its trough is wide and bounded by large normal boundary faults, which developed during the Miocene. The major escarpment between the rift floor and the flanking southern and northern Ethiopian plateaus is built by steep NE striking normal boundary faults and the relative displacement reaches overall differences in height of up to 2000 m (Gebregzabher 1986; Corti 2008). Today the boundary faults are considered to be inactive. A study of their morphology east of Aluto volcano by Pizzi et al. (2006) suggests a tectonically induced rather than a magma-induced faulting. Strain accommodation by mechanical stretching and formation of large border faults is typical for the young stages of rifting and is currently observed in the southern part of the EARS (Kendall et al. 2006). The rift floor in the central MER is dominated by a network of active NNE-SSW oriented faults (Fig. 1). It is the youngest part of the MER and is referred to as Wonji fault belt (WFB).

An intense tectonic event occurred in the Pleistocene-Holocene in the main Ethiopian Rift related to the Wonji Fault (Mohr, 1967). With the formation of the Wonji Fault Belt, tectonic movements and volcanic activity produced step-like structures and associated volcanic activity, represented by ignimbrites, basalts and unwedded pyroclastics. The fault zone is straddled by central volcanoes disposed along the axial zone of the Wonji Fault Belt. The main products were rhyolite, trachyte lava flows, pumice, unwedded tuffs, obsidians and pitch stones. The products of the Wonji fault are referred as Wonji Group (Kazmin at al., 1978 and others). Another type of volcanic activity in Wonji Fault Belt was the eruption from fissures of Pleistocene to Recent basalt lava flows. The basalts are controlled by extensional fractures and commonly characterized by fresh aa surface. Chains of scorraceous cones follow the lines of fractures. These basalts are mostly found in the rift floor; south of lake Ziway and lake Shalla. Recent flows in many cases follow pre-existing topographic low relief areas. Although the development of the rift was dominated by volcanic activity, sedimentation also occurred. Wonji Group rocks are intimately associated with lacustrine sediments related to the ancestral lake in the rift floor in the Pleistocene-Holocene times. Lithologies comprised in the study area are in Pleistocene-Holocene age. Since the mapping area is conducted in the Central Segment of the rift floor, associated volcanic products are recent. Un welded pumice cover the southern parts, lacustrine sediments are widely exposed in the northern and northwestern parts of the study area (Fig. 3). Recent basaltic lava flows and basaltic hyaloclastites are exposed due South of Lake Shalla. Vesiculated welded ignimbrites mostly cover the central and eastern parts of the area.

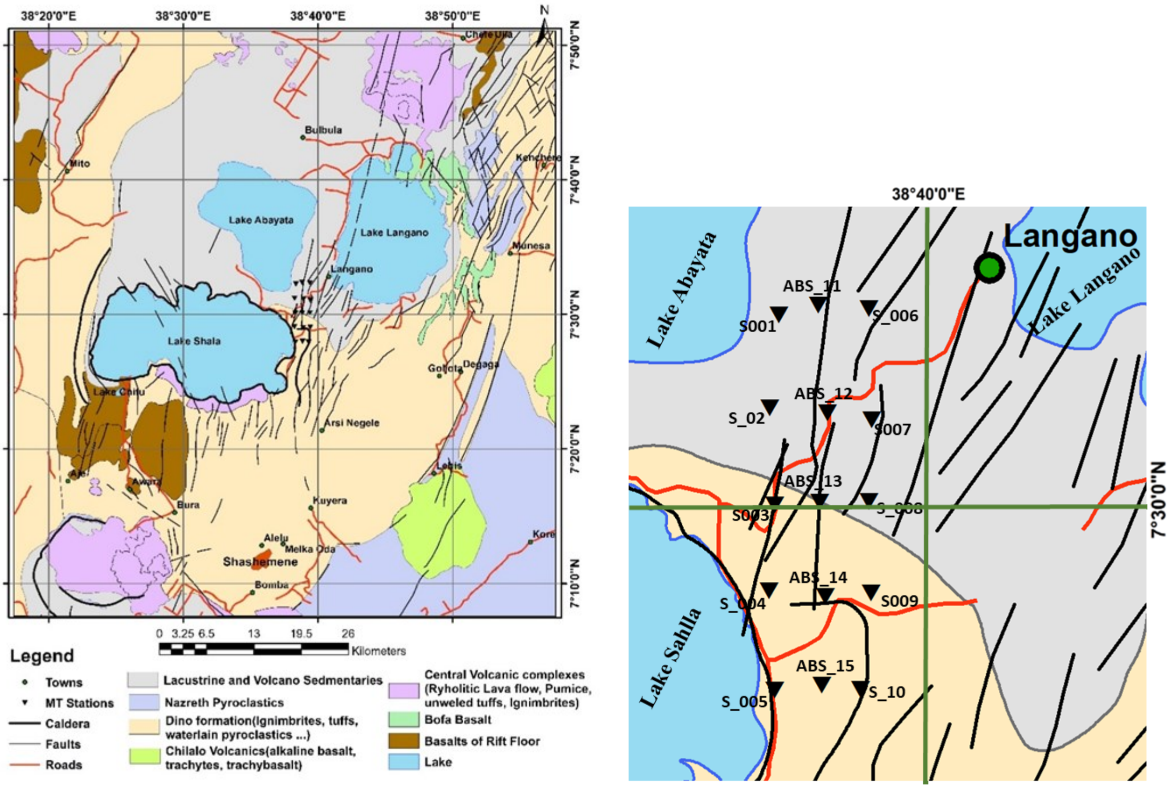

Figure 3: Geological map of Shalla-Abayata geothermal site (left) and MT stations surrounded by lakes (right).

3.DIMENSIONALITY AND DIRECTIONALITY ANALYSIS

Magnetotelluric transfer functions or MT responses are functions that relate the registered electromagnetic field components at a given frequency. There are two magnetotelluric transfer functions. The Impedance Tensors and the Geomagnetic Transfer functions. The impedance tensor describes the relation between the orthogonal electric and magnetic fields of a given frequency. The geomagnetic transfer function, also known as the tipper vector or Tipper, is a dimensionless complex vector showing the relationship between the vertical and the two horizontal components of the magnetic field.

The tipper vector can be decomposed into real and imaginary vectors in the horizontal x-y plane. The real vectors are called induction arrows. In the Wiese convention, the induction vectors point away from lateral increase in electrical conductivity (Wiese, 1962) while in the Parkinson convention (Parkinson, 1959), the vectors point towards lateral increase in electrical conductivity.

Dimensionality and directionality analysis examines how well the data fit the assumed model, and extracts the best fitting regional 1-D or 2-D impedances in the presence of 3-D galvanic distortion. The phase tensor, unaffected by galvanic distortion, provided a practical tool to easily obtain information about the dimensionality (Bibby et al., 2005). Some of techniques that determine the dimensionality and directionality of the electrical conductivity structures are skew, ellipticity, and strike direction.

Swift Skew is skew of impedance matrix rotationally invariant parameter indicating the dimensionality of the subsurface structure (Swift, 1967). The values are less than 0.2 for 1-D and 2-D structures (Swift, 1967). Higher skew values indicate a more complex structure of the site. Some of the results of Swift skew show that greater than 0.2 after 10 s and most of the skew result shows less than 0.2, indication of 1-D/2-D structures (Fig.4).

Bahr skew (BS) is a measure of the local 3-D distortion of regional 2-D fields based on impedance phase, rather than on impedance magnitudes, which is the conventional definition of skew. For BS greater than 3, the data should be considered 3-D and the regional 2-D indicator is below 3 (Bahr, 1991). The BS result around 10 s is greater than 3 showing the 3-D character whereas most part is less than 3, showing the 1-D/2-D character (Fig. 5). The ellipse color filled indicates the BS and at 10 s, the BS increase comparing to other periods (Fig.6). This could be interpreted as showing the 3-D character and also more elliptical than other periods, probably the 3-D effect. The strike direction is also dominated around these periods. If the ellipse looks circle, the data has 1-D/2-D effect.

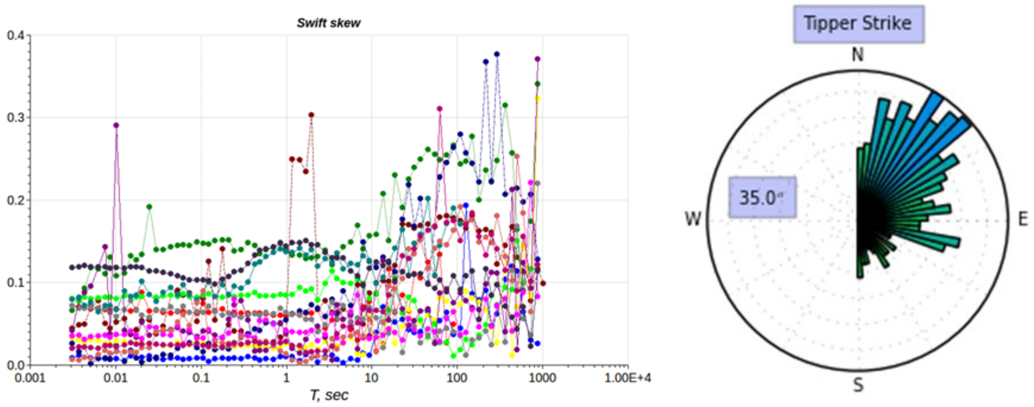

Figure 4: All MT data of Swift skew results of the study area (left) and the induction arrow or the tipper strike direction for all periods (right).

The phase tensor can be represented graphically as ellipses, providing information about the dimensionality of the geo-electrical structure. The phase of the impedance element describes the phase shift between the electric and magnetic field components Caldwell et al. (2004).

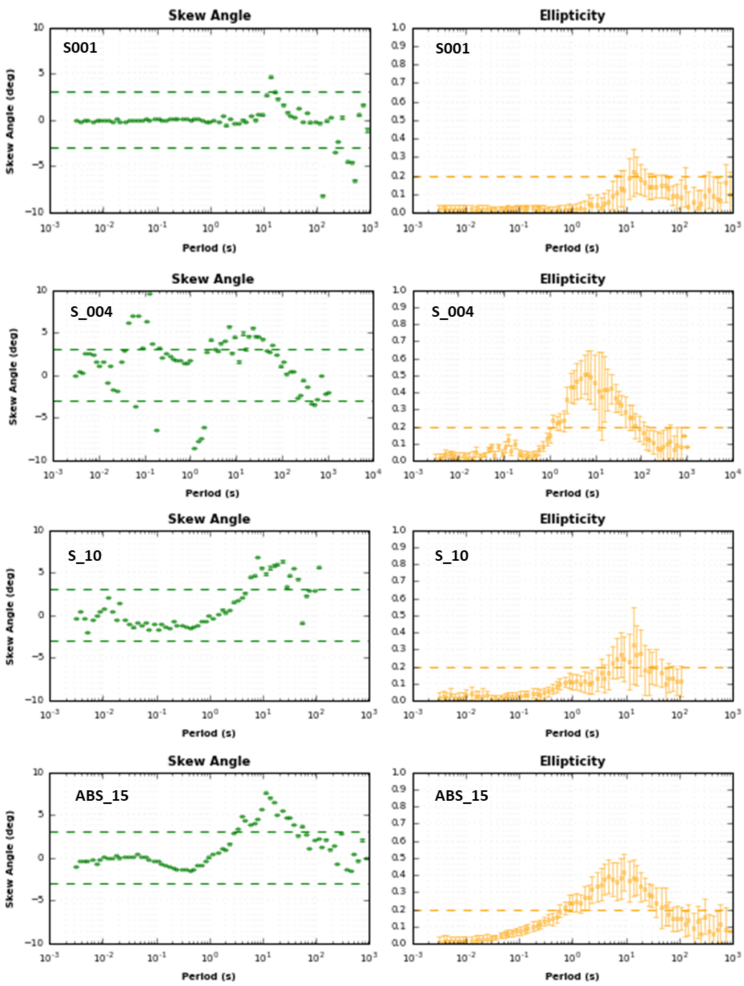

Figure 5: Bahr sensitivity skew of some of the MT data (left) and the ellipticity of the rotationally invariant of the impedance tensor (right).

The major axis of the ellipse at 10 s aligned in NE direction. In the Wiese convention, (Wiese, 1962) was used in which the real induction arrows point away the conductive zone of northeast and north part of the study area through depth. The induction arrows at 0.09 s and 1 s were very small magnitude, indicating that the horizontal resistivity contrast is minor at shallow depth. This suggest that, at this period, the structure is almost 1-D. At 10 s and 100 s, the arrows are longer and point toward SE, probably the dominant place for strike direction and consistent with the occurrence of a geothermal reservoir. For long periods, the induction arrows point to the same direction, this could be related to a large resistive structure at depths of several kilometers (Fig. 6).

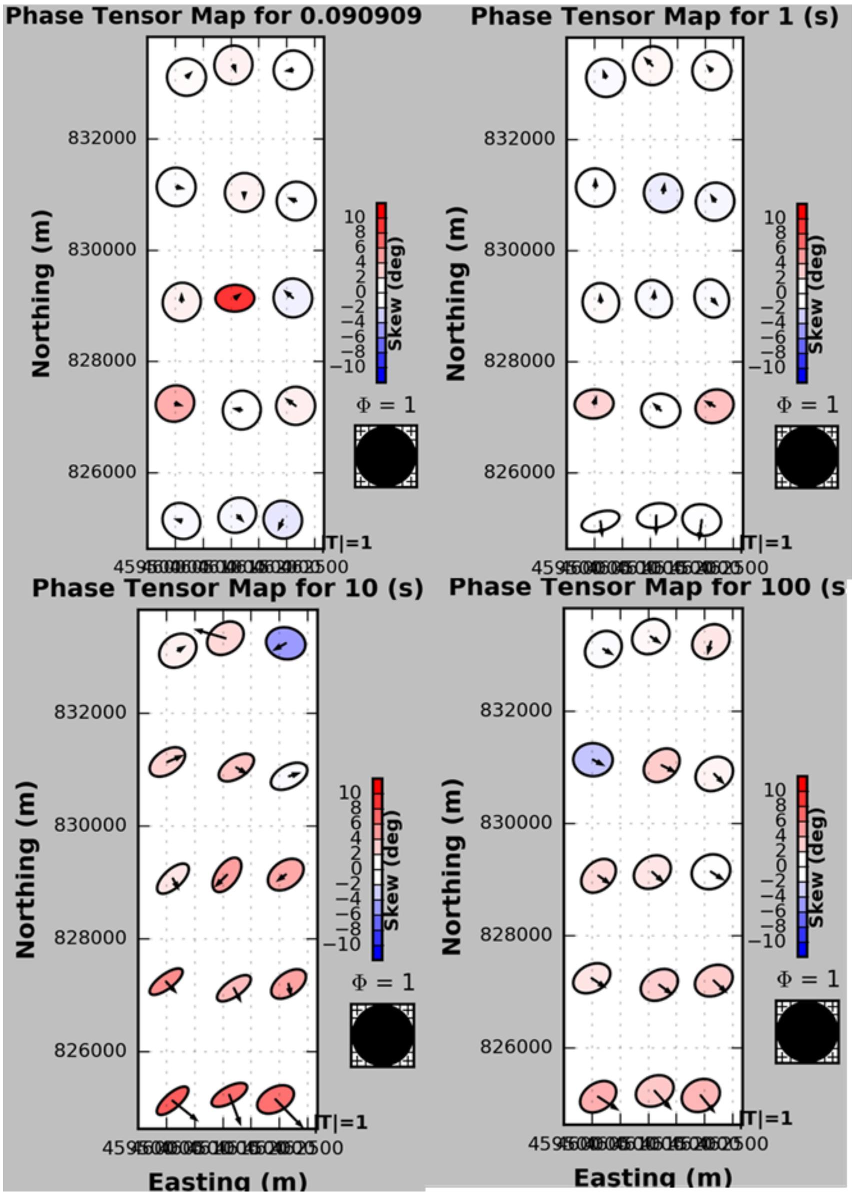

Figure 6: Phase tensor ellipse and real induction arrows at four different periods colored by β angle (phase sensitivity skew).

Figure 7 shows the geoelectrical MT phase tensor pseudo-section (Caldwell et al., 2004) between 0.003-1,000 s for the data used in the inversion. The minimum principal phase color values used to indicate dimensionality, values exceeding 45^o indicate a decrease of resistivity from 0.009 s to around 1 s (interpreted as clay cap with alteration minerals) and from 100 s to 1,000 s (probably interpreted as partial melt), whereas values less than 45^o indicate an increase in resistivity between 1 s to 100 s. This can be interpreted with the unaltered volcanic rocks, probably chlorite as a heat source for the geothermal system.

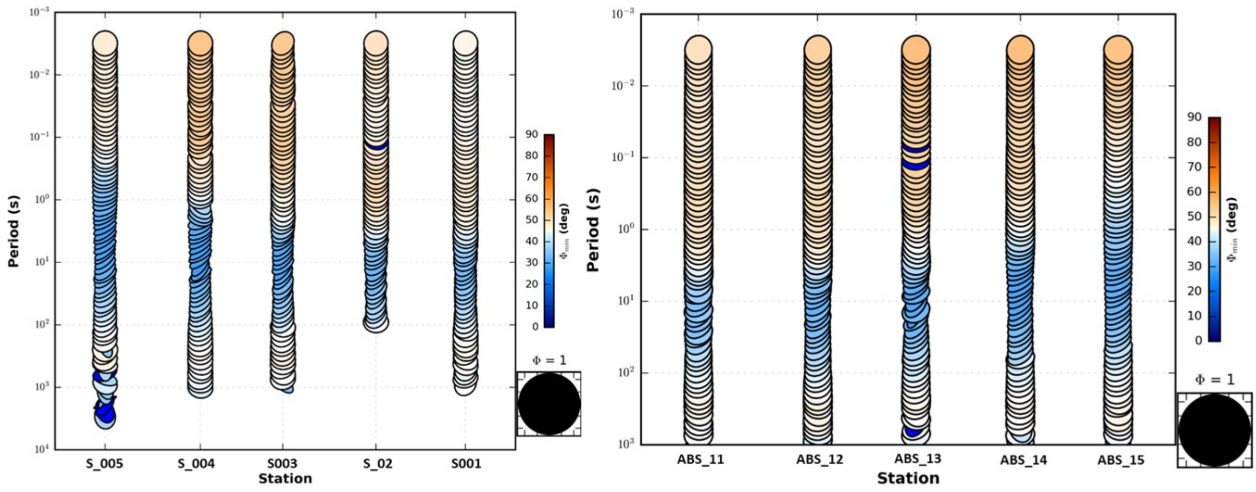

Figure 7: Elliptical representations of phase tensor pseudo-sections for some stations. The ellipses are shaded by the minimum phase angle, with angles greater than 45° indicating a decrease in resistivity with depth, and angles less than 45° representing an increase in resistivity with depth.

Strike direction can be found by making strike direction analysis of the MT data (Zhang et al., 1987). All the invariants of the MT data induction arrow (Wiese, 1962; Parkinson, 1959) show that the regional strike direction is N 35° E direction (Fig. 4). The MT data rotated to strike direction (N 35° E) to minimize the off diagonal elements. In 2D modelling, the azimuth of profile should be perpendicular to the strike direction so that the profiles have to projected 55^0 east to north.

4. RESULT AND DISCUSSION

In Shalla-Abijata geothermal field 15 MT sounding were collected by Geological Survey of Ethiopia. The MT data period range is 0.003 to 1000 s and Occam inversion is used for 2-D modelling. For a 2-D Earth, electrical conductivity is constant along one horizontal direction (along strike) and Maxwell's equations separate into TE (E-polarization) and TM (H-polarization) modes. The joint inversion of the TE and TM mode data along profiles approximately perpendicular to the strike of the structure are performed.

The dimensinality analysis result of the MT data shows that 1-D/2-D character for swift skew for most period ranges as well as Bahr skew. The ellipse looks circle in the periods between 0.009 to 1 s and above 100 s, indicating 1-D/2-D effect but around 10 s, indicates 3-D effect. The minimum principal phase color values used to indicate dimensionality in the phase tensor pseudo-section. Values exceeding 45° indicate a decrease of resistivity from 0.009s to around 1 s correlated altered volcanic rocks zeolite smectite clay alteration mineral and from 100 s to 1,000 s has low resistivity, whereas values less than 45° indicate an increase in resistivity between 1 s to 100 s. This can be interpreted with the unaltered volcanic rocks, probably chlorite as a heat source for zone of up-flow and hottest part of the geothermal field characterized by high temperature.

Most of calculated and measured pseudo-sections are good fitted showing the inversion result is well displayed the resistivity structures and model (Fig. 9). The 2-D resistivity distribution of Shalla-Abyata geothermal field is shown in Figure 8.

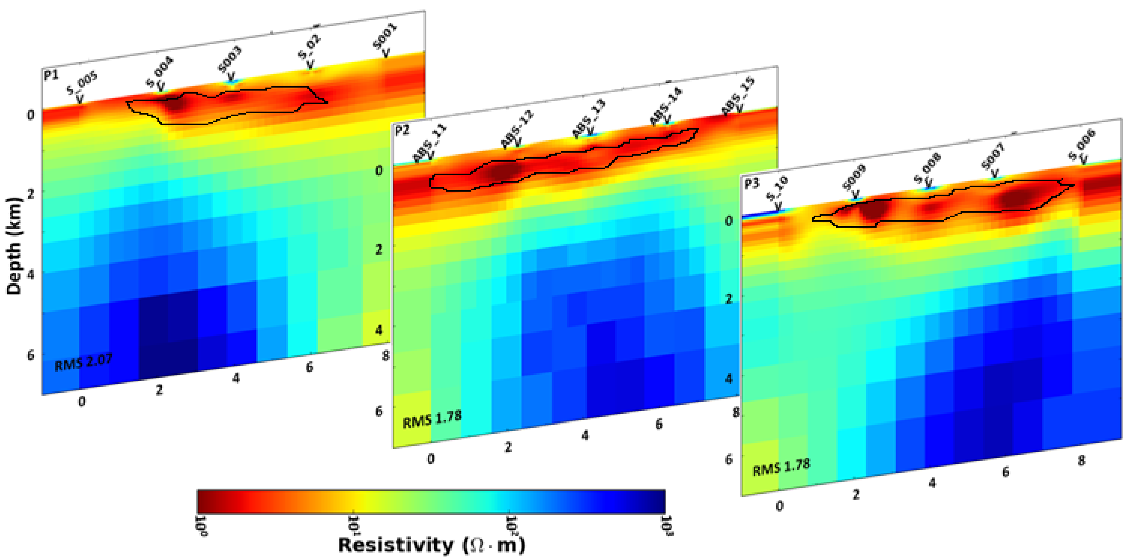

Figure 8: 2-D inversion result using both TE and TM modes for profiles (P1 – P3), the black circles are probable cap rocks.

The 2-D resistivity model produced along the profile using Occam's inversion. The 2-D model reveals similar resistivity structures trend observed in conceptual model high enthalpy geothermal system. Three main resistivity layers are recognized from the 2-D model: a shallow depth relatively high-resistivity layer around the stations (100 Ωm), a conductive layer with resistivity below 10 Ωm, the third resistive zone with high resistivity value (> 100 Ωm).

A conceptual model for high-enthalpy systems by Johnston et al., (1992) and Cumming and Mackie, (2007) describes the temperature pattern, alteration zones and resistivity distribution. The unaltered zone is a region where the hot geothermal fluid does not affect the rocks near the surface and the temperature is low. The unaltered rocks in this region show a high resistivity value in the hundreds of Ωm. This unaltered rock most probably volcanic rocks intercalated with ignimbrite. The existence of clay minerals, especially smectite makes the region below the resistive unaltered layer very conductive. In the region, the temperature is between 70 ^{0}C to 200 ^{0}C and the most common alteration products are smectite and illite. Probably this low resistive anomaly should be lacustrine sediment together with un-welded pumice pyroclastics. The up-flow permeable region below the conductive clay zone is considered the geothermal reservoir in such high-enthalpy geothermal systems and is characterized by high resistivity due to the formation of secondary minerals like chlorite and epidote. This resistive anomaly probably could be the basaltic volcanic rocks. In Fig. 8, the black circle in the inversion model probably the cap rock. Since the MT data has 3-D character around 10 s period and limited data, most of the result is precondition. Further study is required in the study area.

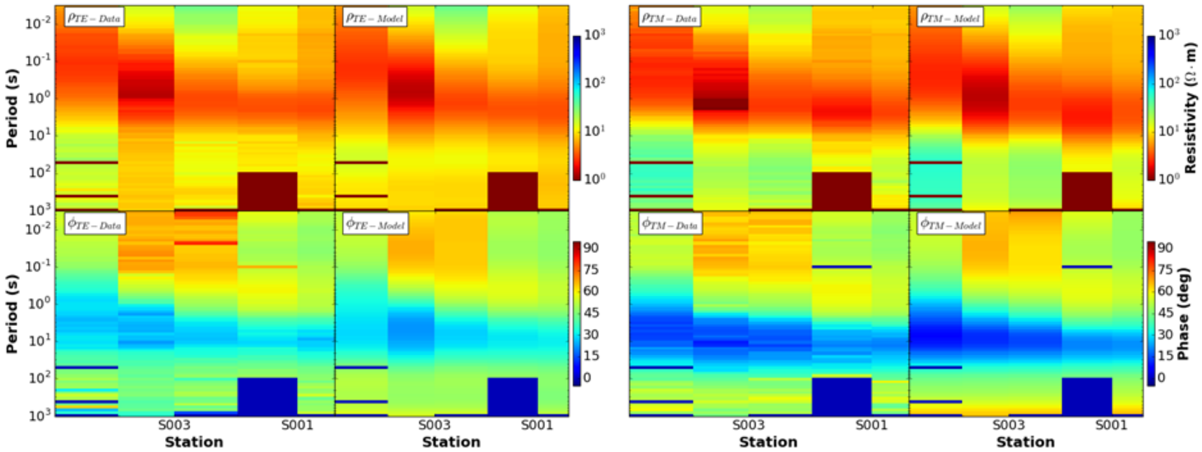

Figure 9a: The Pseudosection plots of observed and calculated response of apparent resistivity and phase along the profile (P1).

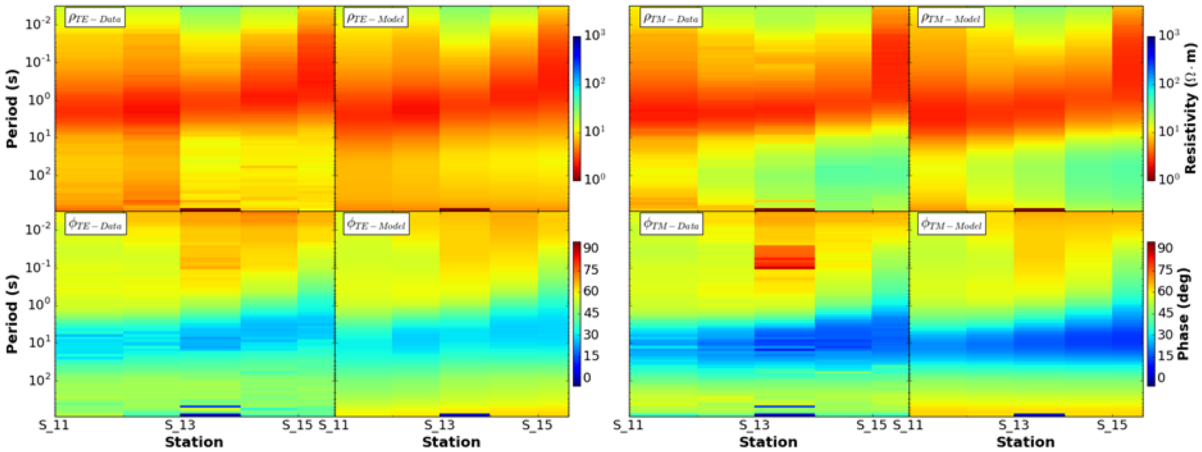

Figure 9b: The Pseudosection plots of observed and calculated response of apparent resistivity and phase along the profile (P2).

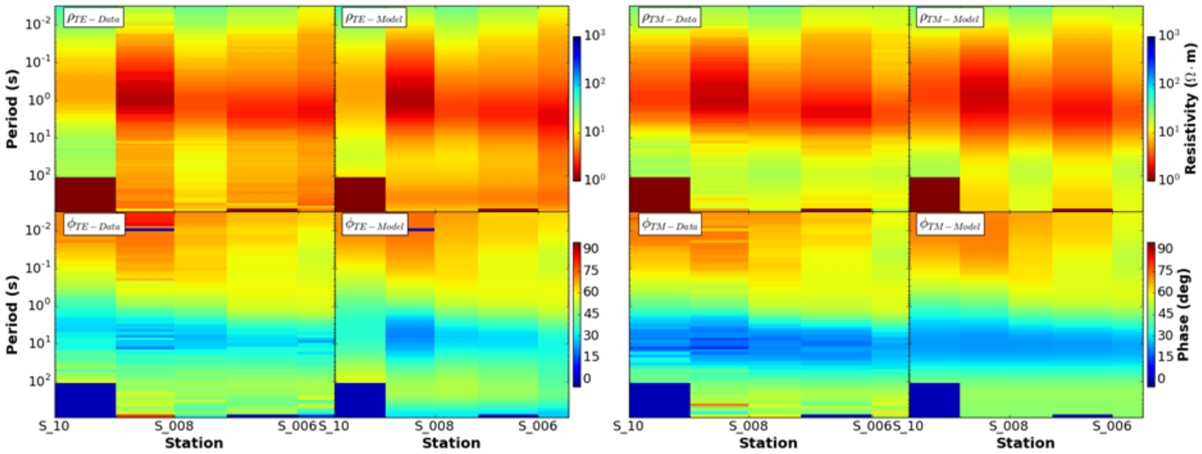

Figure 9c.: The Pseudosection plots of observed and calculated response of apparent resistivity and phase along the profile (P3).

5. CONCLUSION

The dimensionality result and the 2-D inversion model reveals the Shalla-Abayata geothermal field has their subsurface resistivity structure. The high resistivity layer around the stations (100 Ωm) at shallow depth, a conductive layer underneath the high resistive zone with resistivity values below 10 Ωm, and a high resistivity region at deeper depths with resistivity values (> 80 Ωm). In a high-enthalpy geothermal system, the resistivity distribution is highly dependent on the hydrothermal alteration. The alteration zones identified in Aluto-Langano geothermal field at recently drilled wells are similar to the conceptual model. The shallow-high resistivity layer is associated with the fresh volcanic rocks in the unaltered zone with low temperature, where the alteration is minimum. The conductive layer related to the argillic alteration zone due to the formation of conductive alteration minerals, particularly smectite. The resistivity increases gradually at depth beneath the conductive region and is associated with the formation of high-temperature alteration minerals, particularly chlorite and epidote. The inversion result has similar trend with Aluto-Langano geothermal field. Further study is recommended together with drilling in the Shalla-Abijata geothermal field to get enough information. Specially, the deep high resistive chlorite mineral has seen in the southern part of the MT data in the model.

REFERENCES

Agostini, A., Bonini, M., Corti, G., Sani, F. & Manetti, P., 2011. Distribution of quaternary deformation in the central Main Ethiopian Rift, East Africa, Tectonics, **30**(4), doi:10.1029/2010TC002833.

Bahr, K., 1991: Geological noise in magnetotelluric data: classification of distortion types, *Phys. Earth Planet. Inter.,* **66**, 24–38.

Bibby, H. M., Caldwell, T.G., and Brown, C., 2005: Determinable and non-determinable parameters of galvanic distortion in magnetotellurics, Geophys. J. Int., **163**, 915–930.

Caldwell, T.G., Bibby, H.M., Brown, C., 2004. The magnetotelluric phase tensor. *Geophys. J. Int.,* **158**, 457–469.

Constable, S. C., Parker, R. L. and Constable, C. G. (1987). Occam's inversion: A practical algorithm for generating smooth models from electromagnetic sounding data. Geophysics, **52**, 289 – 300.

Corti, G., 2008. Control of rift obliquity on the evolution and segmentation of the Main Ethiopian Rift, Nat. Geosci., **1**(4), 258–262.

Corti, G., 2009. Continental rift evolution: from rift initiation to incipient break-up in the Main Ethiopian Rift, East Africa, Earth-Sci. Rev., **96**(1), 1–53.

Cumming W., and Mackie, R. (2007). 3D MT resistivity imaging for geothermal resource assessment and environmental mitigation at the glass mountain KGRA, California, GRC Transactions, 31, 331–334.

Egbert G. D. (1997), Robust multiple-station magnetotelluric data processing. Geophys. J. Int., **130**, 475–496, doi:10.1111/j.1365-246X.1997.tb05663.x.

Gebregzabher, Z. (1986). Hydrothermal alteration minerals in Aluto Langano geothermal wells, Ethiopia, Geothermics, **15**, 735–740.

Johnston, J., Pellerin, L. & Hohmann, G., 1992. Evaluation of electromagnetic methods for geothermal reservoir detection, TransactionsGeothermal Resources Council, **16**, 241–245.

Kazmin, V.; Berhe, S.M. (1978): Geological map of Nazreth Sheet, Scale 1:250,000, Geological Survey of Ethiopia, Addis Ababa.

Kendall, J., Pilidou, S., Keir, D., Bastow, I., Stuart, G. & Ayele, A., 2006. Mantle upwellings, melt migration and the rifting of Africa: insights from seismic anisotropy, Geological Society, London, Special Publications, **259**(1), 55–72.

Mohr, P.A., (1967). Major volcano-tectonic lineament in the Ethiopian Rift System. Nature, **213**, 664-665.

Parkinson, W.D., 1959. Direction of rapid geomagnetic fluctuations. Geophys. J. R. Astron. Soc., **2**, 1-14.

Pizzi, A., Coltorti, M., Abebe, B., Disperati, L., Sacchi, G. & Salvini, R., 2006. The Wonji fault belt (Main Ethiopian Rift): structural and geomorphological constraints and GPS monitoring, Geological Society, London, Special Publications, **259**(1), 191–207

Smirnov, M.Yu., 2003. Magnetotelluric data processing with a robust statistical procedure having a high breakdown point, Geophys. J. Int., **152**, 1–7.

Swift, C.M., 1967: A magnetotelluric investigation of electrical conductivity anomaly in the southwestern United States, PhD thesis, Massachusetts Institute of Technology, Cambridge, MA.

Vozoff, K. (1991). The magnetotelluric method. In: M. N. Nabighian (ed), Electromagnetic Methods in Applied Geophysics, volume 2 - Application, chapter 8, Society Exploration Geophysicists, 641-711

Wiese, H., 1962. Geomagnetische Tiefentellurik, Teil 2, Die Streichrichtung der Untergrundstrukturen des elektrischen Winderstandes, ersclossen aus geomagnetischen Variationen, Geofis. Pura. Appl., **52**, 83-103.

Zhang, P., Roberts, R.G. and Pedersen, L.B., 1987: Magnetotelluric strike rules. *Geophysics,* **52**, 267–278.